New continuous total ozone, UV, VIS and PAR measurements at Marambio 64°S, Antarctica

Kaisa Lakkala[1,2], Margit Aun[1,3], Ricardo Sanchez[4], Germar Bernhard[5], Eija Asmi[1,4], Outi Meinander[1], Fernando Nollas[4], Gregor Hülsen[6], Veijo Aaltonen[1], Antti Arola[1], and Gerrit de Leeuw[1]

[1]Finnish Meteorological Institute, Climate Research Programme
[2]Finnish Meteorological Institute, Space and Earth Observation Centre
[3]University of Tartu, Estonia
[4]Servicio Meteorológico Nacional, Argentina
[5]Biospherical Instruments, Inc, US
[6]Physikalisch-Meteorologisches Observatorium Davos, World Radiation Center, Switzerland

Correspondence to: Kaisa Lakkala (kaisa.lakkala@fmi.fi)

Abstract. A GUV multifilter radiometer was set up at Marambio, 64°S 56°W, Antarctica, in 2017. The instrument measures continuously ultraviolet (UV) radiation, visible (VIS) radiation and photosynthetically active radiation (PAR). The measurements are designed for providing high quality long-term time series which can be used to assess the impact of global climate change in the Antarctic region. The quality assurance includes regular absolute calibrations and solar comparisons performed

5 at the site and at Sodankylä, Finland. The actual measurements continue the time series measured at Marambio with NILU-UV radiometers during 2000–2010 as part of the Antarctic NILU-UV network. They are optimal for assessing the effects of the ongoing stratospheric ozone recovery on the ecosystem as the data products include information on radiation at various wavelengths ranging from UV to VIS so that changes on biologically effective radiation due to ozone can be separated from those due to other factors. The final data products are total ozone, PAR, VIS radiation at 555 nm, UV index, UV irradiance at

10 5 channels, UVB and UVA dose rate/daily dose, and biologically weighted UV dose rate/ daily dose, including 10 different action spectra. The data from the last five days and the daily maximum UV index time series are plotted and updated daily on the web page fmiarc.fmi.fi/sub_sites/GUVant/. The first two years of UV measurements were very different in terms of the results: The monthly average of daily maximum UVB dose rates were clearly higher in 2018 than in 2017 during the period from October to December. The largest difference was observed in October, when the average of daily maximum UVB dose

15 rates was 7.6 kWm^{-2} and 10.2 kWm^{-2} in 2017 and 2018, respectively. The monthly averages were close to each other for all the three months in 2018, while in 2017 the monthly average of October was lower than those of November and December. VIS and PAR time series show that daily maxima in 2018–2019 exceed those in 2017–2018 during the late spring and the summer (mid-November – January). The studied dataset is freely accessible at http://doi.org/10.5281/zenodo.3553634 (Lakkala et al., 2019).

1 Introduction

The Antarctic area suffers from the well-known springtime ozone hole since the late 1970s (e.g., Farman et al., 1985; WMO, 1990). Increase of harmful UV radiation reaching the surface was expected, as the stratospheric ozone layer protects the Earth from the most dangerous ultraviolet (UV) wavelengths. The international Montreal Protocol was signed in 1987 to restrict
5 the use of ozone depleting substances and thus protect the whole ecosystem from excessive UV levels. The shortest UV wavelengths are known to cause skin cancer, sunburn and cataract, and they can also harm plants, animals and materials.

The Spanish-Finnish-Argentinean Antarctic NILU-UV network was established in 1999/2000 to monitor UV radiation, photosynthetically active radiation (PAR) and total ozone in the Antarctic area and to serve the multidisciplinary UV research community (Lakkala et al., 2008). The NILU-UV multifilter radiometer measurements stopped due to degradation of the
10 instrument at Marambio and other stations in 2013, but they provide reference time series for the severe Antarctic ozone hole period. Between years 2000–2010 the UV index at Marambio reached a maximum of 12 when the station was inside the ozone hole (Lakkala et al., 2018b).

The latest Scientific Assessment of Ozone Depletion (WMO, 2018) suggests that the Montreal Protocol has been successfully adapted and the Antarctic ozone hole has started to recover even though it continues to occur each year. To detect the
15 recovery and its effects on UV radiation and the ecosystem, the Finnish Meteorological Institute (FMI) and the Servicio Meteorológico Nacional Argentina (SMN) started UV and total ozone measurements with multifilter GUV radiometers at Marambio in 2017. As the stratospheric ozone depletion has influenced both stratospheric and surface climate, e.g., cooling of Antarctic stratosphere and southward shift of mid-latitude rain, and the Southern Ocean temperature and circulation, the recovery is expected to have the opposite effects. However the influence of the ozone recovery on climate and ocean can not be predicted
20 as the influence will depend on the evolution of green house gas concentrations in the atmosphere which is the key driver of future southern hemisphere climate (WMO, 2018).

The total ozone, UV radiation, visible (VIS) radiation and PAR measurements of the GUV multifilter radiometer can be used in research assessing the effects of the ongoing climate change. For example, cloud optical depth can be retrieved using measured irradiances (Bernhard et al., 2005) and, together with the irradiance of the visible channel, cloud optical depth can
25 give information on changes in cloudiness. PAR measurements are directly applicable in studies of the effects of climate change on the photosynthesis of plants, algae and bacteria. Both UV and PAR affect micro-organisms living in Antarctic ice and the Southern Ocean. Changes in the amount of aerosols and pollution as well as changes in sea ice extension or ground albedo are also reflected in both UV and VIS radiation time series.

In 2013, the FMI installed Solar Light 501A radiometers at Marambio to monitor both incoming and outgoing UV radia-
30 tion. The measurements are used to determine local albedo and detect changes in it. They can be used to link the NILU-UV measurement time series to the new GUV measurements as they monitor the erythemally weighted UV irradiance, which was one product of the NILU-UV radiometer measurements and is now one of the GUV radiometer products. The Solar Light 501A data collection system consists of one upward and one downward radiometer, which measure the incoming and outgoing irradiance weighted with the action spectrum for UV induced erythema (McKinlay and Diffey, 1987), which in turn also has a

contribution from the UVA. The radiometer pair is selected to represent as similar spectral and cosine responses as possible, as demonstrated in Fig. 1 of Meinander et al. (2008). The system measures in one minute intervals and saves data automatically.

In this paper, the new UV, VIS, PAR and total ozone measurements at Marambio are described and the quality assurance procedures are discussed. Time series of the first two years of measurements are shown.

2 GUV multifilter radiometer measurements at Marambio

GUV multifilter radiometer measurements were installed at Marambio, Antarctica, in collaboration between the SMN and the FMI, in March 2017. The SMN is responsible for the operation and quality control of the measurements at the station, while the FMI is responsible for the quality assurance, data dissemination and data storage.

2.1 Marambio station

The station of Marambio, 64° 14′ S; 56° 37′ W, was founded in 1969 and contributes to the World Meteorological Organization (WMO) Atmospheric Watch Programme. It is located on an island in the eastern Antarctic Peninsula. The altitude of the station is 198 m above the sea level. The temperature ranges from –30°C in winter to +10°C in summer and the mean monthly temperature in June–July is around –15°C and in December–January around –2°C (e.g., Asmi et al., 2018). The Weddell Sea to the east of the Peninsula is frozen year round. During the winter months the ice may extend to latitudes of around 60°S, also covering the coast of the Marambio island. Snow cover is variable but typically exists throughout the winter and a major part of the summer. Heavy cloudiness and fog are common during the summer months, and heavy winds in the winter can blow the snow away yielding to lifting of dust into the air. The prevailing winds at the station are from southwest and northwest. More information on the site can be found from earlier publications (e.g., Karhu et al., 2003; Asmi et al., 2018).

Previously, UV measurements in Marambio have been conducted with a NILU-UV multichannel radiometer during the years 2000–2013 (Lakkala et al., 2018b), and before that, measurements of erythemal UV radiation were carried out by a biometer Solar Ligth 501 installed in 1996 by SMN. The instrument was calibrated by personnel from the World Radiation Center (WRC) in 2006 and 2010. In 2013 it was replaced by a similar instrument belonging to the FMI, when also a radiometer was installed to measure outgoing solar UV radiation (Meinander et al., 2014). Details about the calibration of the new radiometers can be found in Meinander et al. (2008).

Synoptic observations are performed hourly at the Marambio station and additional weather data is obtained from an automatic station. In addition to the synoptic visual cloud observations, cloud coverage and height in Marambio are monitored since the year 2016 with a ceilometer model CL51 (Vaisala), with 30 second resolution.

Marambio also reports to the World Ozone and UV Data Center (WOUDC) and has additionally programs to monitor greenhouse gas concentrations and various aerosol parameters. The number concentration of aerosol particles larger than 10 nm in radius is measured with a Condensation Particle Counter (CPC) model 3772 (TSI Inc.) installed as a part of the particle size distribution measurement system. Aerosol optical properties at the surface are measured with online instrumentation: scattering with an Aurora 3000 nephelometer and absorption with a Multi-Angle Absorption photometer (MAAP) model

5012 (Asmi et al., 2018). Aerosol chemistry is measured offline from the collected weekly filter samples (see e.g., Asmi et al., 2018). Aerosol optical depth in the atmospheric column is measured with a PFR sun photometer which is part of the GAW-PFR network (Tomasi et al., 2015).

2.2 GUV radiometer

5 The GUV radiometer, model GUV-2511, is a multifilter radiometer manufactured by Biospherical Instrument Inc. (BSI), US. The instrument was purchased to monitor UV, visible and PAR radiation at Marambio. The radiometer includes five channels at wavelengths in the UV and one channel in the visible part of the electromagnetic spectrum. The central wavelengths are at 305, 313, 320, 340, 380 and 555 nm, and the full width at half maximum (FWHM) is around 10 nm. In addition there is a seventh channel which measures PAR in the 400–700 nm wavelength region. Using the combination of different channels
10 offers the possibility to retrieve cloud optical thickness and total ozone column. The instrument is environmentally sealed and temperature-stabilized at 40°C. It has a Teflon-covered quartz cosine collector. The instrument specifications, as provided by the manufacturer, are shown in Table 1. Details of the GUV radiometer and its performance are described in Bernhard et al. (2005).

Table 1. GUV model 2511 irradiance array specifications.

Filter type	Custom low-fluorescence interference
Cosine collector	Teflon -covered quartz
Collector area	2.1 cm diameter
Out-of-band rejection	1×10^{-6}
Angular response	0-5% from $0°$ to $70°$; $\pm 10\%$ from $71°$ to $85°$
Typical Saturation	10^{5} $\mu\mathrm{Wcm}^{-2}$ nm^{-1}
Noise equivalent irradiance	10^{-11} Wcm^{-2} nm^{-1}
Temperature coefficient of the dark Signal	Less than ± 3 $\mu\mathrm{volts}/°\mathrm{C}$
Response Temperature Coefficient	Less than $\pm 0.15°\mathrm{C}$

2.3 Data retrieval and products

15 The sampling rate of the GUV radiometer can be set to 1-20 Hz and one minute averages are automatically recorded using LOGGER data-acquisition software. The software converts raw data into irradiances, which are saved as ascii and Microsoft Access Database formats. The daily data is automatically transferred to an ftp server in the SMN, from which the data is transferred and stored into the FMI's data base. Measurements from the last five days and the daily maximum UV index time series are plotted and updated daily on the web page fmiarc.fmi.fi/sub_sites/GUVant/. Examples of these web plots including
20 UV index, UVB, UVA and PAR radiation are shown in Fig. 1. In addition to routine checks of data transfer, the housekeeping

includes cleaning of the diffusers at least once a week, or more frequently if needed, and checking of the leveling once a month.
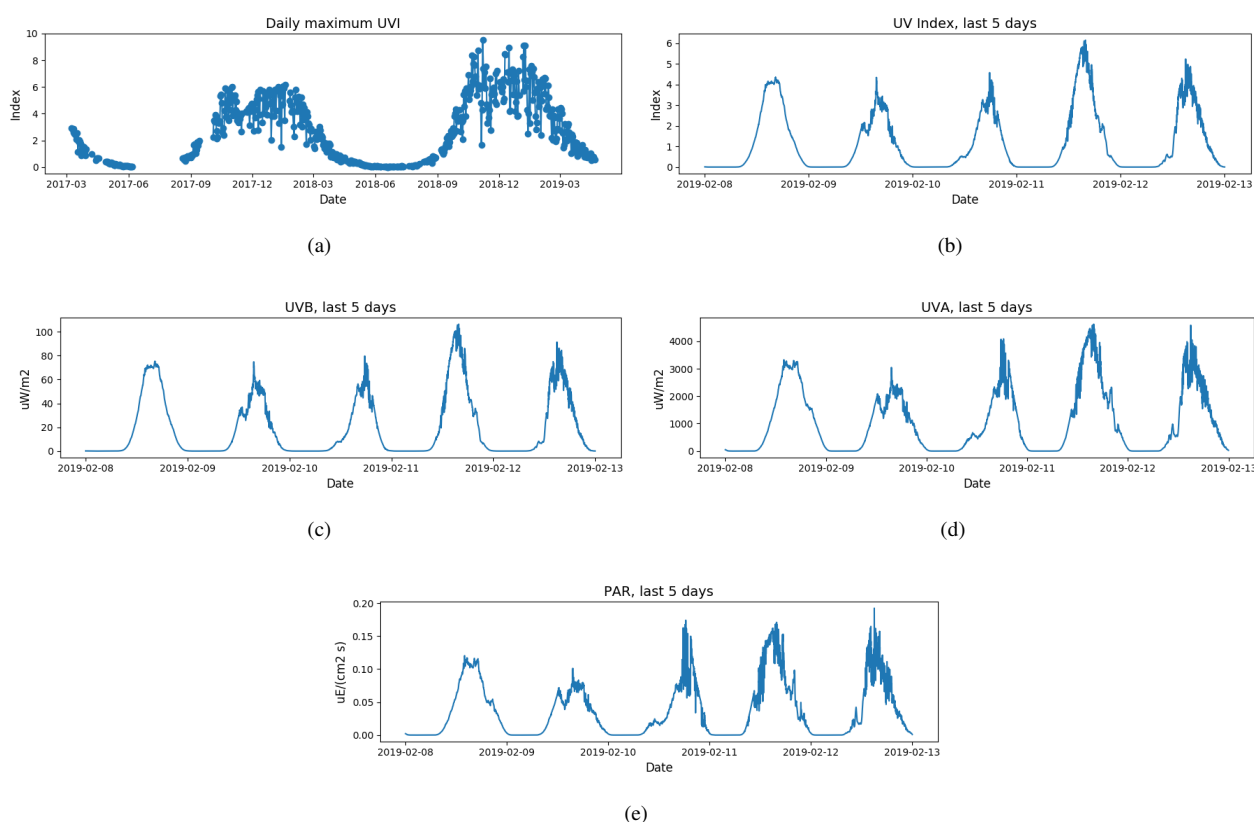
Figure 1. Near real time plots updated daily: A) Daily maximum UV index time series, b) UV index, c) UVB irradiance, d) UVA irradiance and e) PAR. Data in plots b–e are one minute averages.

Near real time data processing includes calculation of data products based on UV, VIS and PAR measurements. The main idea is that each UV product is calculated using a linear combination of calibrated irradiances measured at the five UV channels. The coefficients are determined from solar comparisons between the GUV radiometer and a spectroradiometer following the theory of Dahlback (1996) and Bernhard et al. (2008) as explained in Section 3.1. Bernhard et al. (2005) showed that GUV multifilter UV data was within 3% from data from a well calibrated spectroradiometer for solar zenith angles (SZAs) smaller than 80°. In addition to UV products, VIS radiation and PAR are measured using the 555 nm and 400–700 nm channels, respectively. Total ozone is calculated using lookup tables and the ratio of irradiance measured at 305 nm(a wavelength strongly attenuated by ozone) and 340 nm (a wavelength weakly attenuated by ozone). The complete list of products including several biologically weighted UV dose rates and doses and their references can be found in Table 4.4. of Bernhard et al. (2008). Table 2 summarizes the products calculated from the GUV measurements at Marambio.

Table 2. Data products of the GUV radiometer at Marambio.

Product	Wavelengths [nm] / Biological effect
UV Irradiance	305, 313, 320, 340, 380
UVB and UVA dose rate and daily dose	290–315, 290–320,315–360, 320–360, 360–400, 315–400, 320–400
Visible irradiance	555
Photosynthetically active radiation (PAR)	400-700
UV Index	
Total ozone	
Biologically weighted UV dose rate and daily dose	Erythema, DNA damage, skin cancer in mice, skin cancer in mice corrected for human skin, generalized plant damage, plant growth, damage to anchovy, inhibition of phytoplankton carbon fixation, Inhibition of phytoplankton photosynthesis of phaeodactylum and prorocentrum, inhibition of photosynthesis in Antarctic phytoplankton

3 Quality assurance of the measurements

The quality assurance of the GUV measurements is based on regular absolute calibrations and solar comparisons against high quality spectroradiometers. The FMI has purchased two GUV radiometers in order to avoid gaps in measurement time series. Those two instruments rotate so that one is measuring at Marambio, while the other one is calibrated and compared against
5 reference instruments. Solar comparison is performed each time when the instruments are switched, to detect possible drift or jump in the calibration scale.

Solar comparisons against spectroradiometers are performed at Sodankylä 67°N, in Finland. As the site is located at high latitudes, similar to Marambio, the atmospheric path of UV radiation reaching the surface is similar at both locations: long path in the atmosphere due to high SZAs, which means more ozone absorption and scattering than at lower SZAs. Sodankylä can
10 be classified as an Arctic site from the point of view of stratospheric meteorology. This means that, as Marambio, the station can be located inside, outside or at the edge of the stratospheric Arctic polar vortex, and severe spring time stratospheric ozone loss can occur.

Solar comparisons make it possible to use comparable irradiance scales in both Marambio and Sodankylä. For example, by comparing UV levels at the Arctic and Antarctic location, the effect of ozone loss events on UV radiation can be studied.

15 ### 3.1 Absolute calibration

Both GUV-2511 radiometers (serial numbers #162 and #163) were vicariously calibrated at BSI in April 2016 against measurements of a SUV-100 spectroradiometer that is part of the NSF UV Monitoring Network (Booth et al., 1994). GUV and SUV instruments were installed side by side on the roof platform of BSI in San Diego, California. The SUV-100 measures spectra

of global irradiance between 290 and 600 nm with a spectral resolution of 1 nm. The GUV radiometer with serial number 163 was recalibrated at BSI in April/May 2019 using the same approach.

The calibration method is identical to the method described in Section 4.3 of Bernhard et al. (2008). The procedure is based on the work by Dahlback (1996). In brief, uncalibrated, dark signal corrected measurements of each channel of the GUV

5 radiometers are regressed against cosine error corrected measurements of the SUV-100 spectroradiometer. Measurements of the SUV-100 are weighted with the spectral response functions of the GUV prior to performing the regression. The procedure results in a calibration factor ki for each channel of the GUV. Calibration factor established for GUV #163 in 2016 and 2019 agree to within ±2% with the exception of the channel at 305 nm, which drifted by ±5%. A sensitivity change of this magnitude is not uncommon for a new instrument and typically diminishes over time.

10 Calibrated measurements are finally calculated by dividing the GUVs' raw data with these calibration factors. Measurements of the GUVs' PAR channel are calibrated slightly differently (Bernhard et al., 2008).

Because the SUV-100 data were weighted with the GUV's response functions, calibrated measurements of the GUV are "response-weighted" irradiances (Seckmeyer et al., 2010). The conversion from response-weighted irradiance to useful data products D, such as spectral irradiance for a given wavelength, erythemal irradiance, or the UV index, is performed with the

15 method suggested by Dahlback (1996). In brief, D is approximated by a linear combination of the dark signal corrected signals of the GUVs' UV channels V_i:

$$D = \sum_{i=1}^{5} a_i I_i, \tag{1}$$

where the coefficients a_i depend on the calibration factors k_i and the action spectrum of the biological effect of interests (e.g., erythemal response). The coefficients are determined by solving a system of linear equations as described by Bernhard

20 et al. (2008), taking into account the conditions at the deployment site (e.g., range of total ozone and surface albedo). A comprehensive validation of the conversion method can be found in the paper by Bernhard et al. (2005).

Total ozone column is calculated from GUV measurements with lookup tables, which relate total column ozone to SZA and the ratio of GUV measurements at 305 and 340 nm. The retrieval algorithm is similar to the method described by Stamnes et al. (1991). Lookup tables are calculated with the radiative transfer model UVSPEC/libRadtran (Mayer and Kylling, 2005)

25 and resulting model spectra are weighted with the GUV response functions at 305 and 340 nm. On average, GUV total ozone data agree with OMI data to within ±5% for SZA smaller than 75°. At larger SZA, differences become greater due to the dependence of the retrieval on the vertical distribution of ozone in the atmosphere. Also noise in the GUV 305 nm channel affects the ability to calculate total ozone with good precision at large SZAs. A systematic comparison of GUV and TOMS total ozone measurements at several sites was performed by Bernhard et al. (2005).

30 **3.2 Comparisons against spectroradiometers at Sodankylä**

The GUV radiometer measurements were compared against high quality spectroradiometer measurements during each Northern Hemisphere summer since 2016 (Table 3). The comparisons were performed at the measurement platform next to the sounding station of the FMI Arctic Space Centre in Sodankylä. The FMI has two Brewer spectroradiometers, which routinely

measure UV spectra about every half hour (Mäkelä et al., 2016). The measurements are cosine error corrected (Lakkala et al., 2018a) and the irradiance scale is traceable via the National Standard Laboratory MIKES, Aalto University, Finland, to the scale maintained by the National Research and Testing Institute (SP) (Heikkilä et al., 2016; Lakkala et al., 2008). As the measurement of a Brewer UV spectrum takes around 3 minutes while the GUV radiometer records irradiances averaged over one
5 minute, the three minutes averages of GUV measurements were used in the comparison. UV indices calculated from Brewer #37 spectra and from GUV irradiances were compared and results are shown as function of SZA in Fig. 2.

The first comparison was made in August 2016, right after the radiometers were purchased and before the first one was sent to Marambio. For SZAs lower than 60°, UV indices measured by both GUV radiometers agreed within 1% of each other and the Brewer spectroradiometer. After the comparison, the GUV radiometer #163 was sent to Antarctica and continuous
10 measurements started there in March 2017.

The GUV radiometer #162 stayed in Sodankylä and was compared with the Brewer UV indices during the next years, in June 2017 and July 2018. The sky was clear from clouds during the comparisons. UV indices agreed within 3% for SZAs smaller than 60° in 2017. In 2018, the differences ranged from 2 to 6 %, depending on the SZAs. The SZA dependency was due to the non-corrected angular response of the GUV radiometer. Non-perfect leveling might have caused small azimuth dependency in
15 2018.

The portable UV world reference spectroradiometer QASUME from the World Calibration Center for UV (WCC-UV) at the Physikalisch-Meteorologisches Observatorium Davos, World Radiation Center (PMOD/WRC) visited Sodankylä for a site audit in June 2018. QASUME is a double monochromator spectroradiometer, whose solar UV irradiance measurements are traceable to the primary spectral irradiance standard of the Physikalisch-Technische Bundesanstalt (PTB), Germany, (Gröbner
20 and Sperfeld, 2005). The expanded relative uncertainty (coverage factor k=2) of solar UV irradiance measurements is 3.1% for SZAs smaller than 75° (Hülsen et al., 2016). The GUV #162 was measuring on the site during the audit and the ratios of UV indices derived from it's measurements and QASUME's spectra were calculated. The results are shown in Fig. 2. The weather was unstable during the whole week when the comparisons were made, with changing cloudiness and rain. The day with the thinnest clouds was chosen and spectra measured under rapidly changing cloudiness were excluded from the analysis.
25 The results show that the GUV radiometer UV indices were within ±5% from the QASUME UV indices for SZA lower than 60°. Although measurements performed during rapidly changing cloudiness were excluded from the analysis, the influence of changing cloudiness during the Brewer scan can be indentified as the outlier in Fig. 2, at around SZA 56° on 5 June 2018.

Table 3. Solar comparisons at Sodankylä, Finland.

Date	GUV radiometer	Spectroradiometers
August 2016	GUV162, GUV163	Brewer037, Brewer214
June 2017	GUV162	Brewer037, Brewer214
June 2018	GUV162	Brewer037, Brewer214, QASUME Bentham
July 2018	GUV162	Brewer037, Brewer214
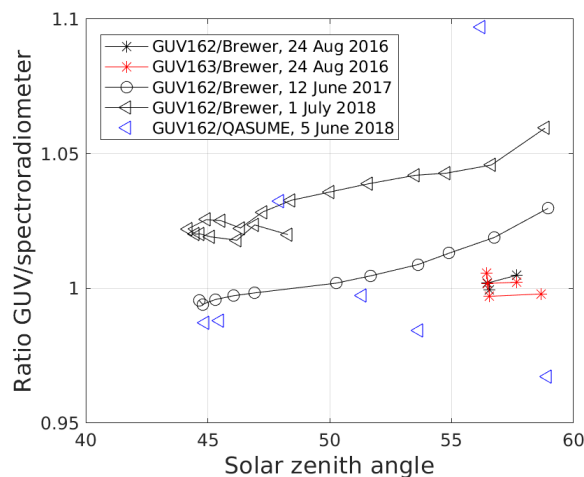
Figure 2. Ratio of the GUVs' and spectroradiometers' UV index at Sodankylä.

3.3   Solar comparison at Marambio

At Marambio, the first switch of the GUV radiometers occurred in November 2018. The GUV #162 was set up next to the GUV #163, which had measured continuously for nearly two years at Marambio. The two instruments measured simultaneously for two weeks before the GUV #163 was packed and shipped for recalibration. The results of the comparison show a difference of 4 – 6% for SZAs smaller than 60° (Fig. 3). Such differences were expected, as it is common for filter radiometers that the wearing-in of Teflon diffuser introduces small changes in the response of channels during the first years of measurements.
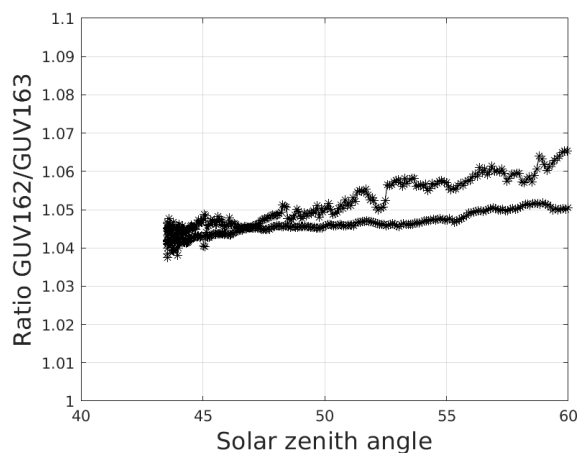
Figure 3. Ratio of the GUVs' UV index at Marambio on 25 November 2018.

4   First two years of measurements

The erythemally weighted UV, maximum UV index and daily average total ozone time series were discussed in Aun et al. (2019) and the results were compared to measurements from other Antarctic measurement sites. In this paper, the time series of noon UV index, noon total ozone, UVB, UVA, VIS and PAR measurements for the period March 2017 – May 2019 are

5   presented in Figs. 4 and 5 (Lakkala et al., 2019). The maximum noon UV indices of the spring–autumn seasons were 6 and 9 in 2017–2018 and 2018–2019, respectively. Noon time UV index refers to the UV index measured at minimum SZA of the day. In 2017–2018, the maximum noon UV index was measured both in the spring (October) and in the summer (January). In 2018–2019 the maximum was measured in the spring when the station was inside the polar vortex (Aun et al., 2019) and exceeded the summer noon maximum UV index which was 8. For the months October – February total ozone was most of

10   the days lower in 2018–2019 than in 2017–2018 (Fig. 4). This resulted in higher UV indices and UVB levels in 2018–2019 compared to the period 2017–2018. The effect of total ozone changes is more pronounced at shorter UVB wavelengths than

(a)

(b)
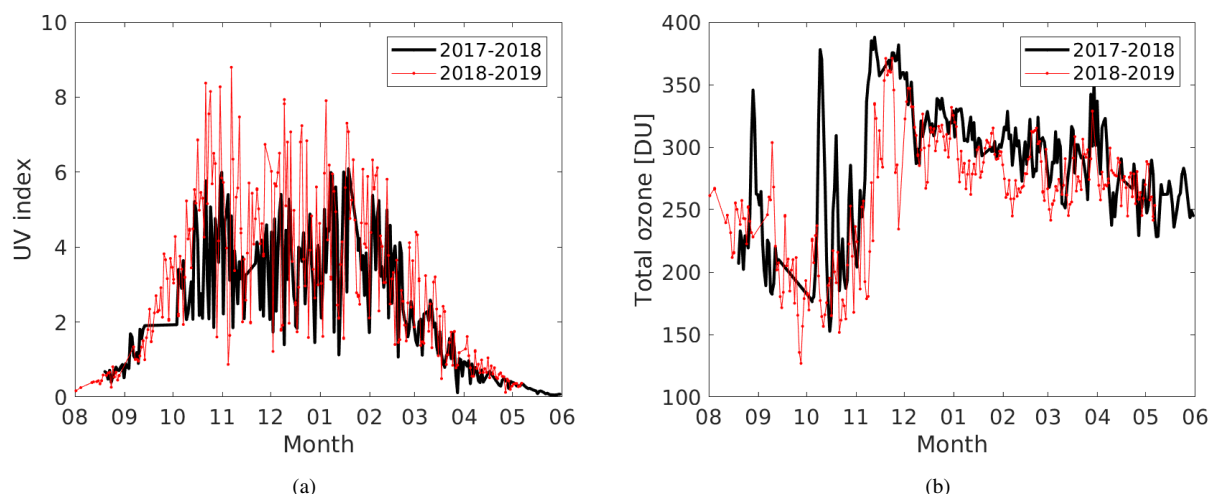
Figure 4. UV index (a) and total ozone (b) at noon calculated from the Marambio GUV radiometer measurements for the months August – May in 2017-2018 and 2018-2019.

at longer UVA wavelengths (Fig. 5), following the ozone absorption spectrum. Elevated UVB dose rates are detected in the spring and in the summer (Fig. 5c). The peak in October–November is due to ozone hole, when the station is located below the stratospheric polar vortex. The reasons for the observed UV features are analyzed and discussed in more detail in Aun et al.

15   (2019).

Variations in VIS and PAR are dominated by variations in cloudiness. Rapidly changing cloudiness is typical in Marambio (Aun et al., 2019), which is seen as high daily variation in all radiation measurements: UV, VIS and PAR. Surface albedo is higher during the spring months than during the summer months, which increases measured radiation in the spring at both shorter UV wavelengths and longer VIS and PAR wavelengths. This results in non-symmetric distribution of daily maxima;

higher spring time VIS radiation and PAR than in the autumn at similar SZAs. The time series of VIS and PAR radiation suggest that there were more cloud-free moments around noon during mid-November – January in 2018–2019 than during the same months in 2017 – 2018, as peaks values where higher during the second year.

Table 4 summarizes the monthly means of the UVB and UVA daily doses, the UVB and UVA daily maximum dose rates,
5 and the VIS and PAR daily maxima for September–March in 2017-2019. The number of measurement days available for daily dose and daily maxima calculations are shown in Tables. 5 and 6, respectively.

Table 4. Monthly means of GUV radiometer products measured at Marambio during the period March 2017 – April 2019. Months with more than 15 measurement days are included. One standard deviation is showed in the parenthesis. DD=daily dose, DMDR = daily maximum dose rate, DM=daily maximum. VIS is irradinace measured at 555 nm.

UVB DD [kJm^{-2}]	Jan	Feb	Mar	Sept	Oct	Nov	Dec
2017	NaN	NaN	16.19(7.06)	NaN	33.55(11.03)	41.38(8.00)	41.53(11.75)
2018	42.62(14.72)	34.60(11.19)	14.09(5.73)	17.74(7.92)	44.04(12.55)	44.89(14.28)	50.56(15.25)
2019	45.86(15.25)	31.62(11.59)	16.36(9.14)	NaN	NaN	NaN	NaN
UVA DD [MJm^{-2}]							
2017	NaN	NaN	0.50(0.20)	NaN	0.78(0.25)	1.18(0.26)	1.04(0.31)
2018	1.04(0.37)	0.91(0.28)	0.45(0.14)	0.45(0.13)	0.89(0.22)	1.04(0.38)	1.24(0.38)
2019	1.08(0.36)	0.79(0.26)	0.51(0.24)	NaN	NaN	NaN	NaN
UVB DMDR [kWm^{-2}]							
2017	NaN	NaN	3.76(1.37)	NaN	7.60(2.25)	8.16(1.26)	9.12(1.98)
2018	9.29(2.47)	7.75(2.06)	3.34(1.36)	4.32(1.82)	10.17(2.80)	10.38(2.96)	10.80(2.45)
2019	9.75(3.34)	7.37(2.60)	3.66(1.84)	NaN	NaN	NaN	NaN
UVA DMDR [kWm^{-2}]							
2017	NaN	NaN	238.90(64.15)	NaN	317.74(69.28)	431.81(59.49)	427.31(92.47)
2018	412.45(117.06)	397.57(89.16)	235.24(65.99)	219.36(33.01)	357.97(77.56)	437.81(134.02)	493.08(108.80)
2019	430.91(141.64)	359.56(96.35)	240.69(81.82)	NaN	NaN	NaN	NaN
VIS DM [mWcm^{-2}nm^{-1}]							
2017	NaN	NaN	75.61(18.85)	NaN	96.16(22.23)	132.00(21.03)	132.10(34.04)
2018	120.14(39.14)	120.72(28.75)	76.18(23.40)	68.39(15.43)	104.92(24.77)	123.58(41.62)	143.86(38.00)
2019	123.36(47.74)	103.05(33.12)	72.73(26.88)	NaN	NaN	NaN	NaN
PAR DM [Em^{-2}s^{-1}]							
2017	NaN	NaN	10.31(2.57)	NaN	13.13(3.04)	18.08(2.87)	17.89(4.50)
2018	16.47(5.38)	16.45(3.80)	10.43(3.17)	9.87(1.44)	14.36(3.38)	17.01(5.73)	19.19(4.87)
2019	16.49(6.26)	14.06(4.41)	9.72(3.61)	NaN	NaN	NaN	NaN

Figure 6 shows ratios of UV irradiances at 305, 313, 320 and 380 nm compared to VIS irradiance at 555 nm in 2017–2018 and 2018–2019. For wavelengths which are affected by ozone absorption (mainly 305 and 313 nm), the spring time low ozone

Table 5. The number of measurement days during 2017-2019 which were available for daily dose calculations. The months from January to December are numbered from 1 to 12.

Year	Month	Number of days
2017	3	22
2017	4	8
2017	8	10
2017	9	13
2017	10	28
2017	11	25
2017	12	29
2018	1	26
2018	2	26
2018	3	31
2018	4	15
2018	8	9
2018	9	25
2018	10	30
2018	11	26
2018	12	31
2019	1	31
2019	2	28
2019	3	27
2019	4	25

episodes are clearly identified as increased ratios (October and November). In the autumn, the radiation path in the atmosphere becomes longer day by day, so that the attenuation of UV radiation is stronger than that of VIS radiation. This is seen at short wavelengths as decrease of the UV/VIS ratio from summer to late autumn. The longer the atmospheric path, the higher the path-integrated total ozone concentration which can absorb UV radiation. The opposite is seen in the spring ratios. UV-A
5   radiation, irradiances at 320 and 380 nm, is only partially absorbed by ozone, and the effect is smaller.

Table 6. The number of measurement days during 2017-2019 which were available for daily maximum calculations. The months from January to December are numbered from 1 to 12.

Year	Month	Number of days
2017	3	22
2017	4	10
2017	5	29
2017	6	5
2017	8	12
2017	9	13
2017	10	28
2017	11	25
2017	12	29
2018	1	26
2018	2	26
2018	3	31
2018	4	23
2018	5	25
2018	6	21
2018	7	21
2018	8	18
2018	9	25
2018	10	30
2018	11	26
2018	12	31
2019	1	31
2019	2	28
2019	3	27
2019	4	30
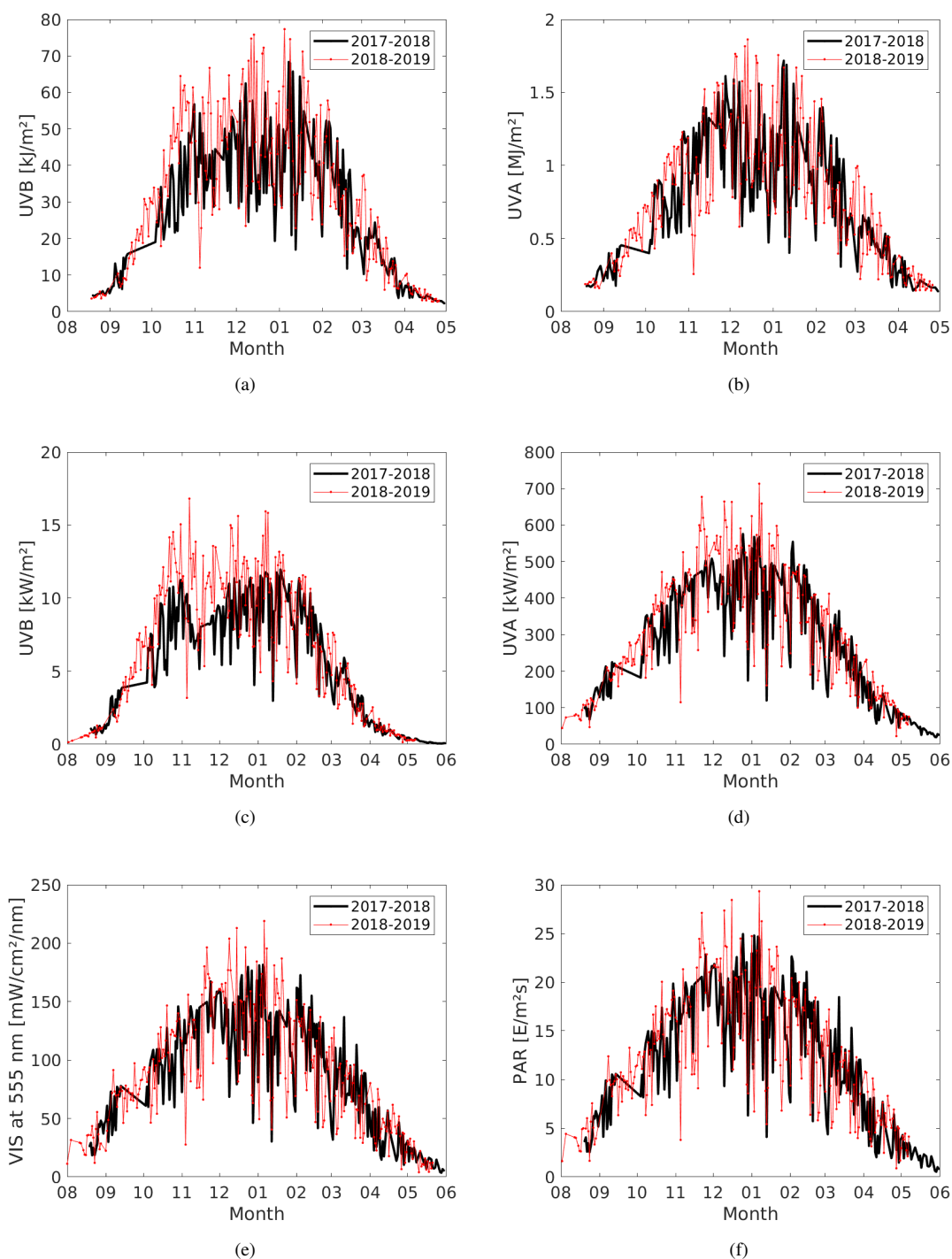
Figure 5. UV and visible radiation time series for the months August – May during periods 2017-2018 and 2018-2019. A) UVB daily dose,
b) UVA daily dose, c)UVB daily maximum, d) UVA daily maximum, e) daily maximum VIS at 555 nm and f) PAR daily maximum.
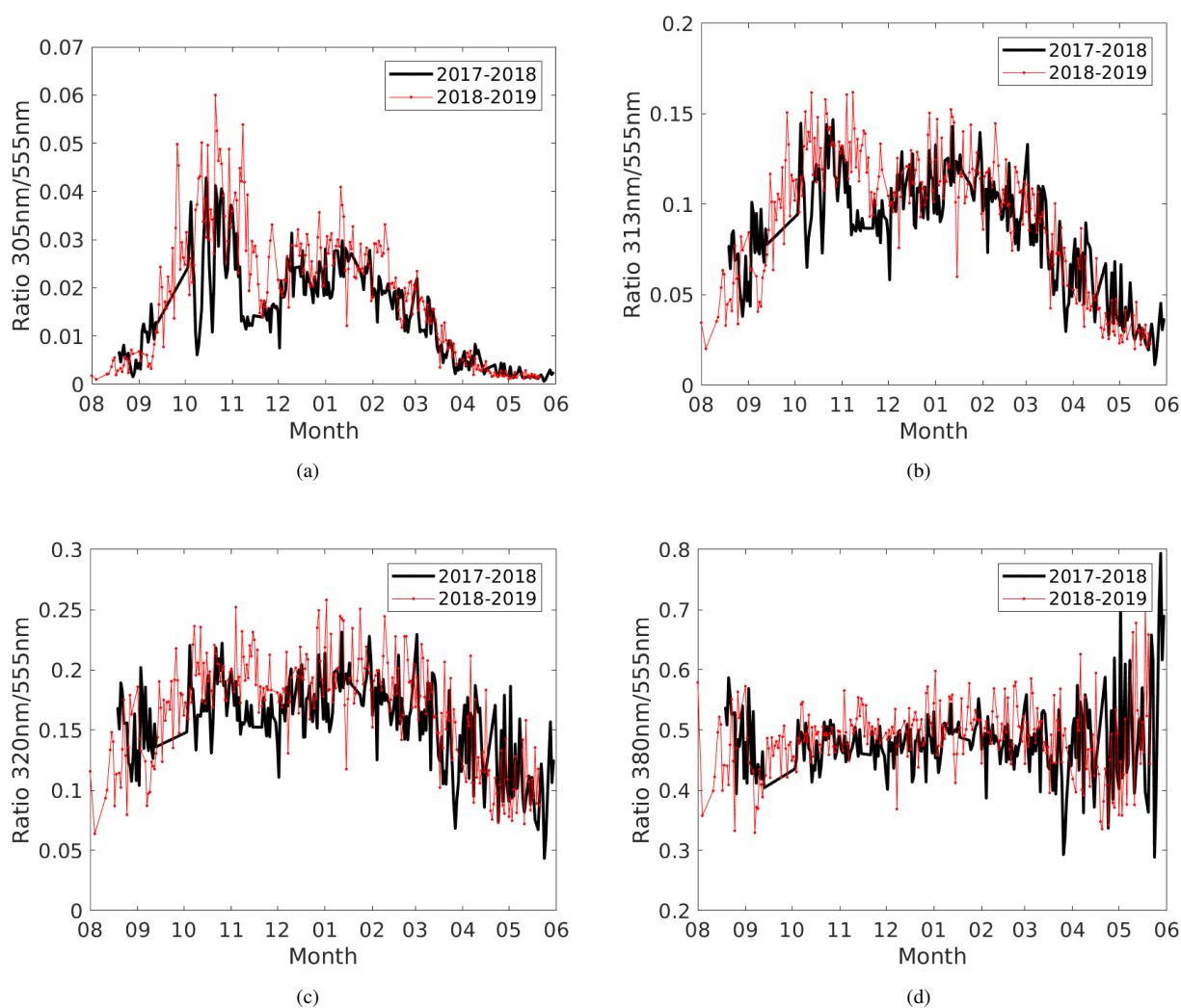
Figure 6. Ratio of daily maximum UV irradiances and VIS irradiances for the months August – May during periods 2017-2018 and 2018-2019. UV irradiances at A) 305 nm, b) 313 nm, c)320 nm and d) 380 nm.

5 Data availability

The studied datasets of UV irradiances, visible and photosynthetically active radiation are freely available at Zenodo, http://doi.org/10.5281/zenodo.3553634 (Lakkala et al., 2019).

6 Discussion and Conclusions

5 Marambio's new GUV multifilter radiometer measurements cover the spectral range from the UV to the VIS, and thus can be used for assessing the spectral effects of changes in factors affecting the amount of solar UV and VIS radiation at the surface: aerosols, albedo, cloudiness and total ozone. Those factors are also influenced by climate change, and thus the measurements serve as important tools for assessing effects of climate change on the Antarctic environment.

The recovery of the stratospheric ozone layer has started (WMO, 2018) and the GUV total ozone measurements will be used

10 to assess features of the recovery in Antarctica. The signs of the recovery can be detected by the UV channels of the radiometer, as actual measurements can be compared with the time series of the Antarctic-NILU-UV network and other UV measurements performed in Antarctica (Aun et al., 2019). The time series of the first two years of GUV measurements show that the recovery is not seen as linear increase in UV levels, and clear differences exist between 2017–2018 and 2018–2019: the effect of the spring time ozone depletion was more pronounced in 2018–2019 than in 2017–2018 with maximum noon UV indices of 9 and

15 6, respectively. This is however far from the maximum UV index measured within the Antarctic NILU-UV network during the years 2000–2010, when maximum UV index 12 was measured at Marambio in the spring (November) 2007 (Lakkala et al., 2018b). For comparison: at Arctic sites the spring time stratospheric ozone loss doesn't increase UV levels to reach the yearly maxima, even during years with severe ozone depletion (Bernhard et al., 2013). In the Arctic, UV index maxima are observed in the summer. For example in Sodankylä, Finland, which is a site affected by stratospheric ozone loss, a maximum UV index

20 of 6 has been measured in the summers of the years 2011 and 2013 (Lakkala et al., 2016).

The Antarctic UV measurements of Marambio can be directly compared to the Arctic UV measurements using the results from solar comparisons between Marambio's GUV radiometer, PMOD-WRC and FMI's spectroradiometers in Sodankylä. The results show that the measurements agreed within $\pm 6\%$ for SZA $< 60°$. These yearly comparisons with Arctic measurements are possible because two GUVs have been purchased for Marambio's measurements: one is measuring at Marambio, while the

25 other is participating in solar comparisons. In addition, regular absolute calibration against high-quality spectroradiometers is part of the quality assurance. The first re-calibration occurred in the spring of 2019. Both solar comparisons and regular absolute calibrations are crucial to obtain homogenized long-term time series, which can serve multidisciplinary research communities. In addition, these high-quality measurements can be used for validation of satellite data, e.g., validation of UV products based on TROPOMI measurements on board the Sentinel-5 Precursor satellite (Lindfors et al., 2018). They are highly valuable, as

30 the ground based measurement network is very sparse at high latitudes.

Ultraviolet radiation products calculated from Marambio's GUV measurements include UV dose rates and doses calculated using 10 different biological action spectra related to UV effects on, e.g., skin, plant, anchovy and phytoplankton. All these UV products can be used when assessing the effects of climate change on the whole Antarctic ecosystem. The effects are not

self-evident even though the melting of ice sheet and snow (e.g., Shepherd et al., 2018) due to temperature increase (Steig et al., 2009) is well recognized. The uncertainty is mostly due to complicated atmosphere-sea-land feedback mechanisms, (e.g., Wang et al., 2019). In future, GUV's VIS radiation time series can be used together with ceilometer measurements and synoptic cloud observations to assess the impact of climate change on cloudiness. Together with the ongoing albedo and aerosol

5   measurements in Marambio they form a complex measurement system for atmospheric radiation studies.

Author contributions. K. Lakkala: Primarily responsible for the QA of the UV data, analyzed the data and led the manuscript preparation.

M. Aun: Programmed GUV data processing for the Marambio station, participated in data analyze and contributed to the writing of the manuscript.

R. Sanchez: Responsible in SMN for Marambio UV measurements. Contributed to the writing of the manuscript.

10   G. Bernhard: Performed the absolute calibration of the GUV radiometers, programmed UV data processing program and contributed to the writing of the manuscript.

E. Asmi: Data analyze of Marambio cloudiness data. Contributed to the writing of the manuscript.

O. Meinander: Responsible for the UV albedo measurements at Marambio. Contributed to the writing of the manuscript.

F. Nollas: Data analyze of Marambio cloudiness data. Contributed to the writing of the manuscript.

15   G. Hülsen: Performed the QASUME site audit in Sodankylä in 2018. Processed QASUME reference UV data.

V. Aaltonen: Responsible for the PFR measurements at Marambio. Contributed to the writing of the manuscript.

A. Arola: Overseeing the work in the group and contributed to the writing of the manuscript.

G. de Leeuw: Group leader during the set up of Marambio UV measurements. Contributed to the writing of the manuscript.

20   *Competing interests.* No competing interests are present.

Acknowledgements. We thank the operators of the GUV radiometers in Marambio. Edith Rodriguez is acknowledged for help with logistics. Hanne Suokanerva and Riika Ylitalo are acknowledged for data dissemination.

References

Asmi, E., Neitola, K., Teinilä, K., Rodriguez, E., Virkkula, A., Backman, J., Bloss, M., Jokela, J., Lihavainen, H., de Leeuw, G., Paatero, J., Aaltonen, V., Mei, M., Gambarte, G., Copes, G., Albertini, M., Fogwill, G. P., Ferrara, J., E., B. M., and Sánchez, R.: Primary sources control the variability of aerosol optical properties in the Antarctic Peninsula, Tellus B: Chem. Phys. Meteorol., 70:1, 1414 571, https://doi.org/10.1080/16000889.2017.1414571, 2018.

Aun, M., Lakkala, K., Sanchez, R., Asmi, E., Nollas, F., Meinander, O., Aaltonen, V., Sogacheva, L., Arola, A., de Leeuw, G., Jakobson, E., De Bock, V., Mangold, A., Bolsee, D., Gillotay, D., Van Opstals, B., Svendby, T., Metelka, L., Cizkova, K., and Disterhoft, P.: UV radiation measurements in Marambio, Antarctica during years 2017–2019 in a wider temporal and spatial context, Atmospheric Chemistry and Physics Discussions, 2019, 1–21, https://doi.org/10.5194/acp-2019-896, https://www.atmos-chem-phys-discuss.net/acp-2019-896/, 2019.

Bernhard, G., Booth, C. R., and Ehramjian, J. C.: Real-time ultraviolet and column ozone from multichannel ultraviolet radiometers deployed in the National Science Foundation's ultraviolet monitoring network, Optical Engineering, 44, 041 011–1–041 011–12, https://doi.org/10.1117/1.1887195, https://doi.org/10.1117/1.1887195, 2005.

Bernhard, G., Booth, C. R., Ehramjian, J. C., and Quang., V. V.: NSF Polar Programs UV Spectroradiometer Network 2006– 2007, Operations Report, 16, Biospherical Instruments Inc., San Diego. Available at http://uv.biospherical.com/report_0607/CHAPTER4.PDF, 2008.

Bernhard, G., Dahlback, A., Fioletov, V., Heikkilä, A., Johnsen, B., Koskela, T., Lakkala, K., and Svendby, T.: High levels of ultraviolet radiation observed by ground-based instruments below the 2011 Arctic ozone hole, Atmospheric Chemistry and Physics, 13, 10 573– 10 590, https://doi.org/10.5194/acp-13-10573-2013, https://www.atmos-chem-phys.net/13/10573/2013/, 2013.

Booth, C., Lucas, T., Mestechkina, T., and Tusson, J.: High resolution UV spectral irradiance monitoring program in polar regions - Nearly a decade of data available to polar researchers in ozone and UV-related studies, Antarctic Journal of the United States - Review 1994, 29, 256–259, 1994.

Dahlback, A.: Measurements of biologically effective UV doses, total ozone abundances, and cloud effects with multichannel, moderate bandwidth filter instruments, Appl. Opt., 35, 6514–6521, 1996.

Farman, J., Gardiner, B., and Shanklin, J.: Large losses of total ozone in Antarctica reveal seasonal CLO_x/NO_x interaction, Nature, 315, 207–210, 1985.

Gröbner, J. and Sperfeld, P.: Direct traceability of the portable QASUME irradiance standard of the PTB, Metrologia, 42, 134–139, 2005.

Heikkilä, A., Mäkelä, J., Lakkala, K., Meinander, O., Kaurola, J., Koskela, T., Karhu, J. M., Karppinen, T., Kyrö, E., and de Leeuw, G.: In search of traceability: Two decades of calibrated Brewer UV measurements in Sodankylä and Jokioinen, Geosci. Instrum. Method. Data Syst., 5, 531, 2016.

Hülsen, G., Gröbner, J., Nevas, S., Sperfeld, P., Egli, L., Porrovecchio, G., and Smid, M.: Traceability of solar UV measurements using the Qasume reference spectroradiometer, Appl. Opt., 55, 7265–7275, https://doi.org/10.1364/AO.55.007265, http://ao.osa.org/abstract.cfm?URI=ao-55-26-7265, 2016.

Karhu, J. A., Taalas, P., Damski, J., Kaurola, J., Ginzburg, M., Villanueva, C. A., Piacentini, E., and Garcia, M.: Vertical distribution of ozone at Marambio, Antarctic Peninsula, during 1987–1999, Journal of Geophysical Research: Atmospheres, 108, https://doi.org/10.1029/2003JD001435, http://dx.doi.org/10.1029/2003JD001435, 4545, 2003.

Lakkala, K., Arola, A., Heikkilä, A., Kaurola, J., Koskela, T., Kyrö, E., Lindfors, A., Meinander, O., Tanskanen, A., Gröbner, J., and Hülsen, G.: Quality assurance of the Brewer spectral UV measurements in Finland, Atmos. Chem. Phys., 8, 3369–3383, 2008.

Lakkala, K., Jaros, A., Aurela, M., Tuovinen, J.-P., Kivi, R., Suokanerva, H., Karhu, J., and Laurila, T.: Radiation measurements at the Pallas-Sodankylä Global Atmosphere Watch station — diurnal and seasonal cycles of ultraviolet, global and photosynthetically-active radiation, Boreal Env. Res., 21, 427–444, 2016.

Lakkala, K., Arola, A., Gröbner, J., León-Luis, S. F., Redondas, A., Kazadzis, S., Karppinen, T., Karhu, J. M., Egli, L., Heikkilä, A., Koskela, T., Serrano, A., and Vilaplana, J. M.: Performance of the FMI cosine error correction method for the Brewer spectral UV measurements, Atmospheric Measurement Techniques, 11, 5167–5180, https://doi.org/10.5194/amt-11-5167-2018, https://www.atmos-meas-tech.net/11/5167/2018/, 2018a.

Lakkala, K., Redondas, A., Meinander, O., Thölix, L., Hamari, B., Almansa, A. F., Carreno, V., García, R. D., Torres, C., Deferrari, G., Ochoa, H., Bernhard, G., Sanchez, R., and de Leeuw, G.: UV measurements at Marambio and Ushuaia during 2000–2010, Atmospheric Chemistry and Physics, 18, 16 019–16 031, https://doi.org/10.5194/acp-18-16019-2018, https://www.atmos-chem-phys.net/18/16019/2018/, 2018b.

Lakkala, K., Aun, M., Sanchez, R., Bernhard, G., Asmi, E., Meinander, O., Nollas, F., Hülsen, G., Aaltonen, V., Arola, A., and De Leeuw, G.: Datasets of UV irradiance, visible and photosynthetically active radiation in Marambio, Antarctica from March 2017 to May 2019 [Data set]., Zenodo. http://doi.org/10.5281/zenodo.3553634, 2019.

Lindfors, A. V., Kujanpää, J., Kalakoski, N., Heikkilä, A., Lakkala, K., Mielonen, T., Sneep, M., Krotkov, N. A., Arola, A., and Tamminen, J.: The TROPOMI surface UV algorithm, Atmospheric Measurement Techniques, 11, 997–1008, https://doi.org/10.5194/amt-11-997-2018, https://www.atmos-meas-tech.net/11/997/2018/, 2018.

Mäkelä, J. S., Lakkala, K., Koskela, T., Karppinen, T., Karhu, J. M., Savastiouk, V., Suokanerva, H., Kaurola, J., Arola, A., Lindfors, A. V., Meinander, O., de Leeuw, G., and Heikkilä, A.: Data flow of spectral UV measurements at Sodankylä and Jokioinen, Geosci. Instrum. Method. Data Syst., 5, 193, 2016.

Mayer, B. and Kylling, A.: Technical note: the libRadtran software package for radiative transfer calculations-Description and examples of use, Atmos. Chem. Phys., 5, 1855–1877, https://doi.org/1680-7324/acp/2005-5-1855, 2005.

McKinlay, A. and Diffey, B.: A reference action spectrum for ultraviolet induced erythema in human skin, in *Human Exposure to Ultraviolet Radiation: Risks and Regulations: Proceedings of Seminar Held in Amsterdam, 23-25 March 1987*, edited by Passchler, W.R. and Bosnakovic, B.F.M., Elsevier, Amsterdam, 83-87, 1987.

Meinander, O., Kontu, A., Lakkala, K., Heikkilä, A., Ylianttila, L., and Toikka, M.: Diurnal variations in the UV albedo of Artcic snow, Atmos. Chem. Phys., 8, 6551–6563, 2008.

Meinander, O., Asmi, E., Neitola, K., Laurila, T., Lihavainen, H., Aaltonen, V., Poikonen, A., Aarva, A., Rodriguez, E., Kyrö, E., de Leeuw, G., Sanchez, R., and Mei, M.: Finnish-Argentinian Measurements on Snow UV Albedo in Marambio, In: FINNARP. Science and Support in Antarctica. Finnish Antarctic Research Program (FINNARP), ISBN 978-951-697-841-6, 2014., 2014.

Seckmeyer, S., Bais, A., Bernhard, G., Blumthaler, M., Johnsen, B., Lantz, K., and McKenzie, R.: Instruments to Measure Solar Ultraviolet Radiation, Part 3: Multi-channel filter instruments, World Meteorological Organization (WMO), Global Atmosphere Watch Report No. 190, 2010.

Shepherd, A., Ivins, E., and et al. (IMBIE team): Mass balance of the Antarctic Ice Sheet from 1992 to 2017, Nature, https://doi.org/10.1038/s41586-018-0179-y, 2018.

Stamnes, K., Slusser, J., and Bowen, M.: Derivation of total ozone abundance and cloud effects from spectral irradiance measurements, Appl. Opt., 30, 4418–4426, https://doi.org/10.1364/AO.30.004418, http://ao.osa.org/abstract.cfm?URI=ao-30-30-4418, 1991.

Steig, E. J., Schneider, D. P., Rutherford, S. D., Mann, M. E., Comiso, J. C., and Shindell, D. T.: Warming of the Antarctic ice-sheet surface since the 1957 International Geophysical Year, Nature, https://doi.org/10.1038/nature07669, 2009.

Tomasi, C., Kokhanovsky, A. A., Lupi, A., Ritter, C., Smirnov, A., O'Neill, N. T., Stone, R. S., Holben, B. N., Nyeki, S., Wehrli, C., Stohl, A., Mazzola, M., Lanconelli, C., Vitale, V., Stebel, K., Aaltonen, V., de Leeuw, G., Rodriguez, E., Herber, A. B., Radionov, V. F., Zielinski, T., Petelski, T., Sakerin, S. M., Kabanov, D. M., Xue, Y., Mei, L., Istomina, L., Wagener, R., McArthur, B., Sobolewski, P. S., Kivi, R., Courcoux, Y., Larouche, P., Broccardo, S., and Piketh, S. J.: Aerosol remote sensing in polar regions, Earth-Science

5 Reviews, 140, 108 – 157, https://doi.org/https://doi.org/10.1016/j.earscirev.2014.11.001, http://www.sciencedirect.com/science/article/pii/ S0012825214001913, 2015.

Wang, Y., Yuan, X., Bi, H., Liang, Y., Huang, H., Zhang, Z., and Liu, Y.: The Contributions of Winter Cloud Anomalies in 2011 to the Summer Sea-Ice Rebound in 2012 in the Antarctic, Journal of Geophysical Research: Atmospheres, 124, 3435–3447, https://doi.org/10.1029/2018JD029435, https://agupubs.onlinelibrary.wiley.com/doi/abs/10.1029/2018JD029435, 2019.

10 WMO: Scientific Assessment of Stratospheric ozone: 1989, World Meteorological Organization (WMO), Global Ozone Research and Monitoring Project–Report No. 20, 1990.

WMO: Scientific Assessment of Ozone Depletion: 2018, World Meteorological Organization (WMO), Global Ozone Research and Monitoring Project–Report No. 58, 2018.